NANO LETTERS

pubs.acs.org/NanoLett Letter

Dynamic Continuum of Nanoscale Peptide Assemblies Facilitates Endocytosis and Endosomal Escape

Hongjian He, Jiaqi Guo, Jiashu Xu, Jiaqing Wang, Shuang Liu, and Bing Xu*

Cite This: *Nano Lett.* 2021, 21, 4078−4085 Read Online

ACCESS | Metrics & More | Article Recommendations | Supporting Information

ABSTRACT: Alkaline phosphatase (ALP) enables intracellular targeting by peptide assemblies, but how the ALP substrates enter cells remains elusive. Here we show that nanoscale phosphopeptide assemblies cluster ALP to enable caveolae-mediated endocytosis (CME) and endosomal escape. Specifically, fluorescent phosphopeptides undergo enzyme-catalyzed self-assembly to form nanofibers. Live cell imaging unveils that phosphopeptides nanoparticles, coincubated with HEK293 cells overexpressing red fluorescent protein-tagged tissue-nonspecific ALP (TNAP-RFP), cluster TNAP-RFP in lipid rafts to enable CME. Further dephosphorylation of the phosphopeptides produces peptidic nanofibers for endosomal escape. Inhibiting TNAP, cleaving the membrane anchored TNAP, or disrupting lipid rafts abolishes the endocytosis. Decreasing the transformation to nanofibers prevents the endosomal escape. As the first study establishing a dynamic continuum of nanoscale assemblies for cellular uptake, this work illustrates an effective design for enzyme-responsive supramolecular therapeutics and provides mechanism insights for understanding the dynamics of cellular uptake of proteins or exogenous peptide aggregates.

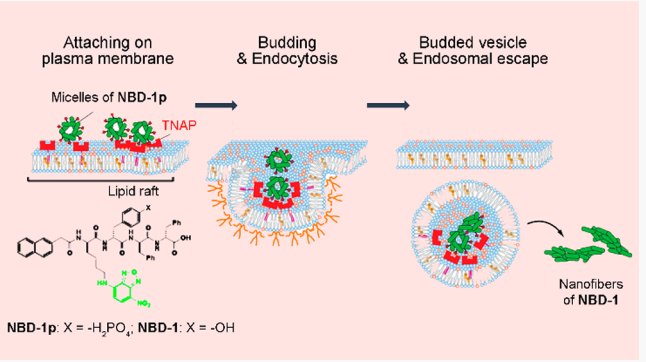

KEYWORDS: *Self-Assembly, Endocytosis, Endosomal Escape, Tissue-Nonspecific Alkaline Phosphatase*

INTRODUCTION

Because many drug targets identified by molecular cell biology are inside cells, considerable efforts have focused on engineering molecules for intracellular delivery of various cargo.[1−3] Besides the use of cationic molecules for enhancing cellular uptake of therapeutics,[4−6] one of the most explored approaches for intracellular delivery is to engineer molecules to be responsive to chemical or physical stimuli, such as redox,[7−10] pH,[11−13] enzymes,[14−23] or light.[24,25] Among the enzymatic approach, alkaline phosphatase (ALP)-instructed self-assembly of peptides is particularly effective to facilitate the cellular uptake of the peptide assemblies.[14−18,26−28] However, the mechanism of this phenomenon is largely unknown. Coincidently, viruses also use a responsive motif for cell entry. For example, the life cycle of a virus (e.g., SARS-CoV-2)[29] begins at the attachment to the plasma membrane of the host cells[30] to clustering plasma membrane-bound receptors, followed by viral proteolytic priming (VPP)[31,32] for endocytosis and endosomal escape. Prompted by the mechanism of viral cell entry, we hypothesize that the assemblies of phosphopeptides, as the substrate of ALP, act as a dynamic continuum[33] to cluster the ALP to facilitate endocytosis and to undergo an enzymatic morphological transition that enables the endosomal escape (Scheme 1). This hypothesis is also based on several additional rationales: (i) ALP is a GPI-anchor protein, and its clustering enables caveolae-mediated endocytosis;[30] (ii) ALP, locating in lipid rafts, plays a key role in the cellular uptake of aberrant protein aggregates; and (iii) ALP-catalyzed dephosphorylation enables morphological transition (e.g., nanoparticles to nanofibers) and generates artificial intracellular filaments.[17]

To prove our hypothesis, we synthesize a phosphopeptide, which, above its critical micelle concentration (CMC), self-assembles to form nanoparticles, which transform into nanofibers upon the dephosphorylation catalyzed by ALP. The phosphopeptide molecules initially aggregate on the plasma membrane to cluster tissue-nonspecific alkaline phosphatase (TNAP) in lipid rafts of HEK293 cells that overexpress TNAP, then enable caveolae-mediated endocytosis (CME). The assemblies of the phosphopeptides gradually change their morphology from nanoparticles to nanofibers depending on the extent of dephosphorylation. Abolishing the interaction between the TNAP and the phosphopeptides

Received: March 13, 2021
Revised: April 28, 2021
Published: May 3, 2021

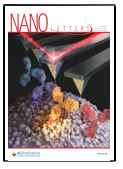

Scheme 1. Illustration of a Dynamic Continuum of Peptide Assemblies for Endocytosis and Endosomal Escape

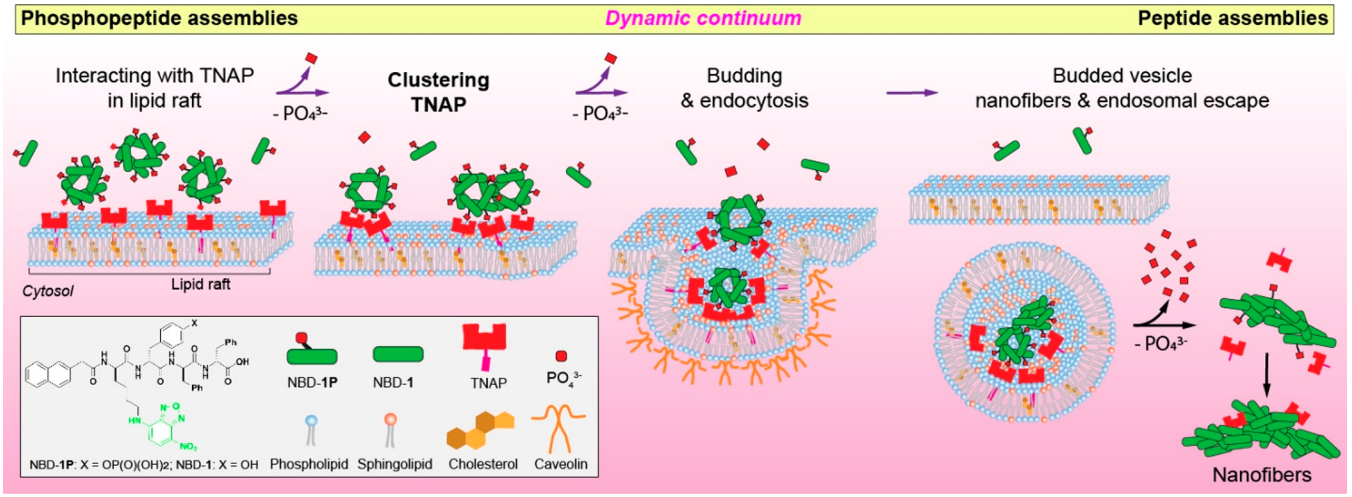

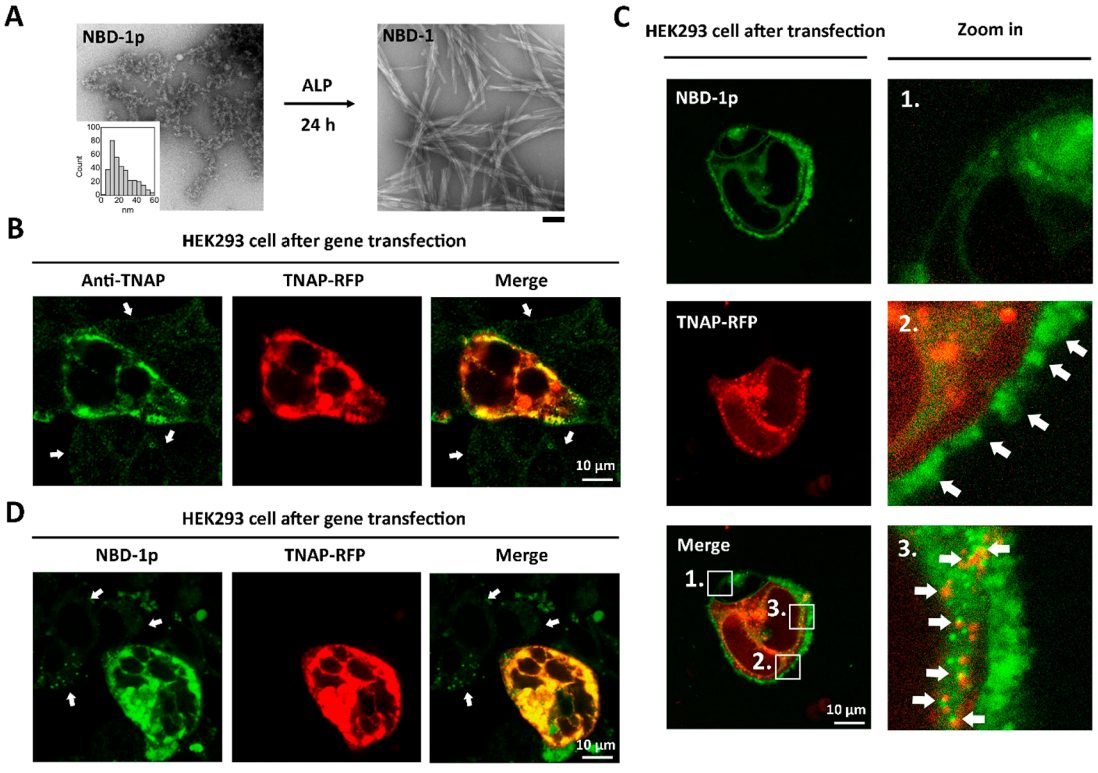

Figure 1. Upregulation of TNAP promotes the endocytosis of phosphopeptide assemblies. (A) TEM images of **NBD-1p** (200 μM) before and after the addition of ALP (0.1 U/mL, 37 °C) for 24 h. The inset is the diameter distribution of the nanoparticles formed by **NBD-1p**. Scale bar = 100 nm. (B) Immunofluorescence staining of TNAP in the transfected HEK293 cell. The nontransfected cells (pointed by arrows) show little TNAP. (C) Confocal fluorescence images of HEK293_TNAP-RFP cells coincubated with **NBD-1p** (200 μM, 5 min, no washing). To visualize **NBD-1p** at an early stage, the laser power here is 5 times stronger than that used in panel D. (D) Confocal fluorescence imaging of TNAP-RFP transfected HEK293 cells treated by **NBD-1p** (200 μM, 12 h, washed). The nontransfected cells (indicated by arrows) show little intracellular NBD fluorescence.

significantly decreases the endocytosis. The TNAP, which remained in the endosome, catalyzes the further dephosphorylation of the phosphopeptides, generating peptide nanofibers to facilitate endosomal escape. As the first study that illustrates the intracellular peptide assemblies resulted from dynamic peptide assemblies rather than from a monomeric peptide or static assemblies, this work not only provides insights for understanding the cellular uptakes of proteins or exogenous peptide aggregates but also offers the guidance for designing enzyme-responsive supramolecular assemblies as intracellular targeting therapeutics.[34]

RESULTS AND DISCUSSION

Scheme 1 shows the structure of the fluorescent phosphopeptide (**NBD-1p**). For studying the cellular uptake of the phosphopeptides, a nitrobenzoxadiazole (NBD), as the fluorophore, conjugates to the side chain of the D-lysine in a naphthyl capped D-phosphotetrapeptide (D-Lys-D-pTyr-D-Phe-

https://doi.org/10.1021/acs.nanolett.1c01029
Nano Lett. 2021, 21, 4078−4085

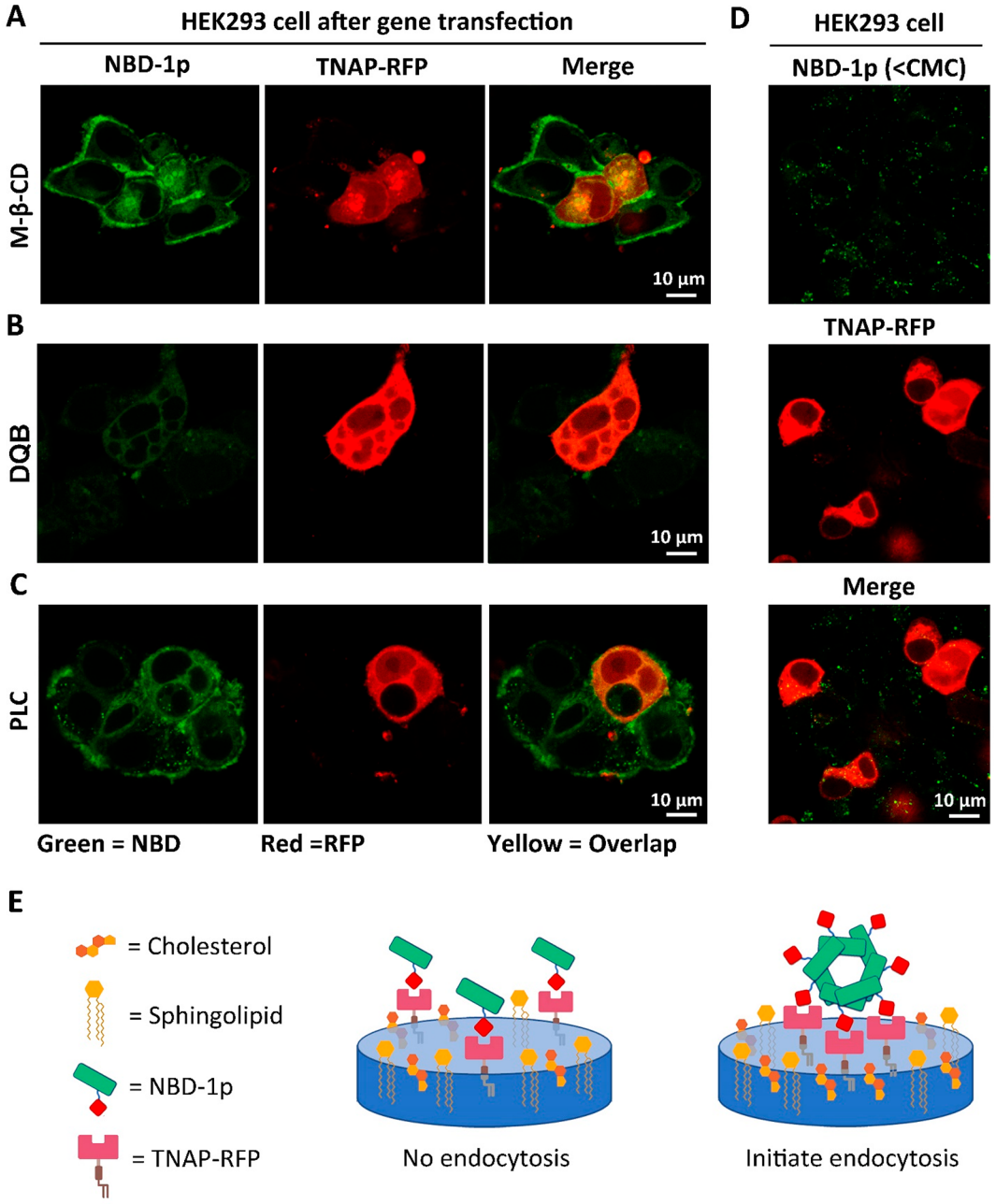

Figure 2. NBD-1p nanoparticles associate with the TNAP in lipid rafts followed by CME. (A−C) Confocal fluorescence images of HEK293_TNAP-RFP cells incubated with **NBD-1p** (200 μM, 12 h) after the pretreatment of (A) caveolin-dependent endocytosis inhibitors (M-β-CD), (B) a TNAP inhibitor (DQB), and (C) phospholipase C which removes the GPI-anchored TNAP on plasma membrane. (D) Confocal fluorescence images of HEK293_TNAP-RFP cells incubated with **NBD-1p** (50 μM, 12 h) below CMC. (E) Illustration of that the assemblies of phosphopeptide rather than individual molecules initiate CME.

D-Phe). Using an Fmoc-based solid-phase peptide synthesis, we first produced this naphthyl capped D-phosphopeptide and then conjugated it to NBD. Then, the purification by high performance liquid chromatography (HPLC) produces the designed **NBD-1p**. Transmission electron microscopy (TEM) reveals that **NBD-1p** monomers primarily self-assemble into nanoparticles (22.4 ± 7.2 nm in diameter, Figure 1A) at 200 μM (PBS, pH = 7.4), which is above its critical micelle concentration (CMC, 159 μM, Figure S1). Upon the addition of ALP for catalytically dephosphorylating **NBD-1p**, the nanoparticles formed by **NBD-1p** transform into short nanofibers (21.9 ± 3.7 nm in diameter and about 300−1000 nm in length) made of **NBD-1** (Figure 1A and Scheme S1). This result confirms that **NBD-1p** undergoes enzyme-instructed self-assembly.[35]

We choose HEK293 cells for testing our hypothesis because of their constitutively low expression of ALP, reliable growth, and propensity for transfection.[36] Treating HEK293 cells with the polyethylenimine (PEI)[37] carrying the DNA plasmid encoding red fluorescent protein-tagged TNAP (TNAP-RFP), we generate a cell population consists of the HEK293 cells that overexpress TNAP-RFP (Figure 1B, the transfected cells are denoted as HEK293_TNAP-RFP) and the HEK293 cells without gene transfection (Figure 1B, indicated by arrows). To observe the fluorescence of **NBD-1p** at the early stage of endocytosis, we used high laser strength for imaging. Co-

https://doi.org/10.1021/acs.nanolett.1c01029
Nano Lett. 2021, 21, 4078−4085

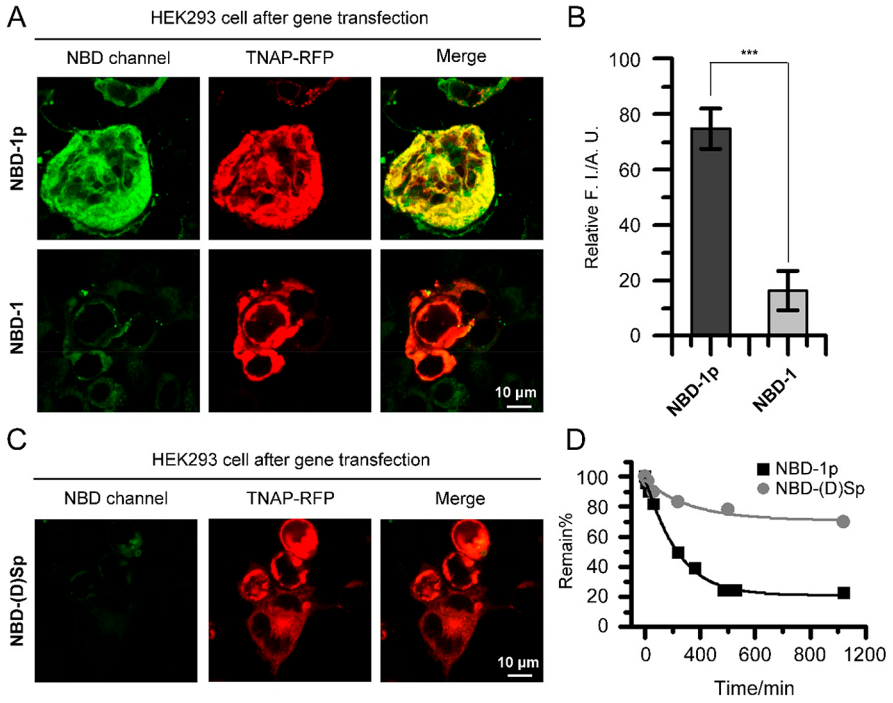

Figure 3. Phosphotyrosine is critical for rapid cellular uptake. (A) Confocal fluorescence images of HEK293_TNAP-RFP cells incubated with **NBD-1p** or **NBD-1** (200 μM, 12 h, washed), respectively. (B) ImageJ analysis of intracellular fluorescence intensity of HEK293_TNAP-RFP cells in panel A. Data is presented as mean ± standard deviation, *** means $p < 0.001$. (C) Confocal fluorescence images of HEK293_TNAP-RFP cells incubated with **NBD-(D)Sp** (400 μM, 12 h, washed). (D) Dephosphorylation rate of **NBD-1p** and **NBD-(D)Sp** by ALP (0.1 U/mL, 37 °C).

incubating **NBD-1p** (above CMC) with the HEK293 cells, after the transfection, reveals that, initially (5 min), **NBD-1p** mainly accumulates on the plasma membrane of HEK293_TNAP-RFP cells in a discrete pattern (Figure 1C, region 2, indicated by arrows), although the phosphopeptides barely interact with the plasma membrane of the nontransfected control (Figure 1C, region 1). The cell selective aggregation of **NBD-1p** on the plasma membrane of HEK293_TNAP-RFP cells indicates that the nanoparticles formed by **NBD-1p** associate with the plasma membrane-bound TNAP[38,39] for dephosphorylation. The interaction between TNAP and the nanoparticles (made of mainly **NBD-1p** and small amount of **NBD-1**) spatially induces the clustering of TNAP on the plasma membrane (Scheme 1). Monomers of **NBD-1p**, being dephosphorylated rapidly, would likely interact with TNAP only briefly. Moreover, we observed not only the formation of more endocytic vesicles in HEK293_TNAP-RFP cells than in the nontransfected control (Figure 1C, regions 1 and 3), but also some vesicles containing TNAP-RFP and **NBD-1p** in HEK293_TNAP-RFP cells (Figure 1C, region 3, and Movie S1). These results suggest that the TNAP-participating endocytosis of **NBD-1p** nanoparticles is enhanced in HEK293_TNAP-RFP cells. While some NBD fluorescence exists in some nontransfected HEK293 cells and the endosomal vesicles lacking TNAP in the transfected HEK293 cells, these NBD signals may originate from the cellular uptake of **NBD-1p** via other endocytosis pathways (e.g., macropinocytosis, a nonspecific endocytosis) and the enhanced intracellular NBD fluorescence or autofluorescence under high laser strength. Nonetheless, other endocytosis pathways, like macropinocytosis, are less likely act as the main path for the phosphopeptide assemblies (Figure S2). Additionally, **NBD-1p** can still enter the nontransfected HEK293 cells via CME, although inefficiently due to low TNAP expression. The intracellular fluorescence from NBD increases significantly over time in the HEK293_TNAP-RFP cells, while remaining mostly unchanged in the nontransfected HEK293 cells (Figure 1D, Figure S3, and Movie S2). Trypan blue hardly stains the HEK293_TNAP-RFP cells with **NBD-1p** (Figure S4), confirming an intact cell membrane. Additionally, after the incubation with **NBD-1p**, the TNAP gene transfected HEK293 cells exhibit lower cell viability than that of the wild type (Figure S5). The cytotoxicity may originate from the formation of intracellular **NBD-1** nanofibers after dephosphorylation. These results confirm that the overexpression of TNAP in the HEK293 cell promotes the cellular uptake of the assemblies of **NBD-1p**.

Further study on the endocytosis of **NBD-1p** nanoparticles shows that pretreating the HEK293 cells (after TNAP transfection) with methyl-β-cyclodextrin (M-β-CD), a CME inhibitor via dissipating lipid rafts on a plasma membrane,[40,41] at the cell compatible concentration (2.5 mM), drastically reduces the cellular uptake efficiency of **NBD-1p** (Figure 2A) compared to the control (Figure 1D). This result indicates that (i) M-β-CD decreases the CME efficiency at that working concentration, and (ii) CME contributes to the cell entry of **NBD-1p** which adheres on the plasma membrane of HEK293_TNAP-RFP cells (Figure 1C, region 2). Since TNAP is enriched in the lipid rafts on the plasma membrane,[42] this result also suggests that the assemblies of **NBD-1p** on the plasma membrane (Figure 1C, region 2) associate with the TNAP in lipid rafts and then cluster the TNAP, which signals the endocytosis of **NBD-1p** through CME[30] (Scheme 1). The CME of **NBD-1p** nanoparticles triggered by TNAP aggregation agrees with the formation of endocytic vesicles containing TNAP-RFP and **NBD-1p** (Figure 1C, region 3). Using 2,5-dimethoxy-*N*-(quinolin-3-yl)-benzenesulfonamide (DQB), a noncompetitive inhibitor of TNAP with an allosteric

https://doi.org/10.1021/acs.nanolett.1c01029
Nano Lett. 2021, 21, 4078−4085

inhibition mechanism,[43] to inhibit the enzymatic reaction (i.e., TNAP catalyzing the dephosphorylation of **NBD-1p**) or the removal of plasma membrane-bound TNAP via phospholipase C (PLC) which cleaves the GPI anchors[44] that link TNAP to plasma membrane also substantially decreases the cellular uptake of **NBD-1p** into HEK293_TNAP-RFP cells (Figure 2B,C). These results further support that the interaction between TNAP and the nanoparticles of **NBD-1p** is important for signaling CME. Below the CMC, the individual **NBD-1p** molecules neither aggregate on the plasma membrane of HEK293_TNAP-RFP cells (Figure S6 and Movie S3) nor enter the cells efficiently (Figure 2D), although the monomeric phosphopeptides may still associate with the TNAP on the cell surface as the substrate of TNAP (Figure 2E). These results indicate that the clustering of TNAP in lipid rafts by the nanoparticles formed by the self-assembly of **NBD-1p** is essential for signaling the CME of the assemblies of **NBD-1p** (Figure 2E).

To further validate that the interactions between TNAP and the D-pTyr in the nanoparticles of **NBD-1p** initiate the CME, we incubated the HEK293_TNAP-RFP cells with **NBD-1** (i.e., the dephosphorylated **NBD-1p**, Scheme S1). Clearly, the HEK293_TNAP-RFP cells treated by **NBD-1** exhibit significantly less intracellular fluorescence intensity than those treated by **NBD-1p** (Figure 3A,B). This result suggests that the interaction between TNAP and D-pTyr plays a role in the CME of the **NBD-1p** assemblies. Replacing the D-pTyr by D-pSer, we generated a derivative of **NBD-1p**, named **NBD-(D)Sp**. The HEK293_TNAP-RFP cells incubated with **NBD-(D)Sp** show drastically reduced cellular uptake of the phosphopeptide compared to the incubation with **NBD-1p** (Figure 3C). The dephosphorylation assay reveals that ALP dephosphorylates **NBD-1p** much faster than **NBD-(D)Sp** at the same concentration (Figure 3D), indicating that ALP exhibits a higher affinity for **NBD-1p** than **NBD-(D)Sp**. The results above suggest that the interaction between ALP and its substrate is necessary for the CME of the phosphopeptides. Moreover, a sequence-scrambled phosphopeptide derivative of **NBD-1p**, denoted as **NBD-2p** (with the sequence of D-Phe-D-Phe-D-Lys(ϵ-NBD)-D-pTyr, Scheme S1), also enters the HEK293_TNAP-RFP cells more efficiently than the non-transfected HEK293 cells (Figure S7). This result indicates that the cellular uptake of the phosphopeptide assemblies containing D-pTyr depends more on the interactions between TNAP and the enzyme triggers than on the binding between receptors and specific peptide sequences.[45−47]

The dispersive fluorescence of **NBD-1p** in HEK293_TNAP-RFP cells (Figures 1D and 3A) confirms not only the endocytosis of **NBD-1p** but also the endosomal escape of the peptide assemblies. Considering the cell entry mechanism of SARS-CoV-2, in which the proteolytic cleavage of S proteins by endosomal proteases (e.g., cathepsin B and cathepsin L) promotes the release of the viral genome from endosome to cytosol,[48] we reckon that, after the CME of the assemblies of **NBD-1p**, further dephosphorylation catalyzed by the TNAP in endosomal compartments induces a phase transition of the peptide assemblies, which facilitates the endosomal escape of NBD-1 into cytosol. Liquid chromatography−mass spectrometry (LC−MS) analysis of the cell lysate of HEK293_TNAP-RFP cells that are preincubated with **NBD-1p** confirms the dephosphorylation of the peptide inside cells (Figure S8). Additionally, TEM images of liposomes encapsulating **NBD-1p** and ALP exhibit the generation of nanofibers that rupture the liposomes (Figure 4A). These results imply that the TNAP in endocytic vesicles converts the **NBD-1p** nanoparticles to

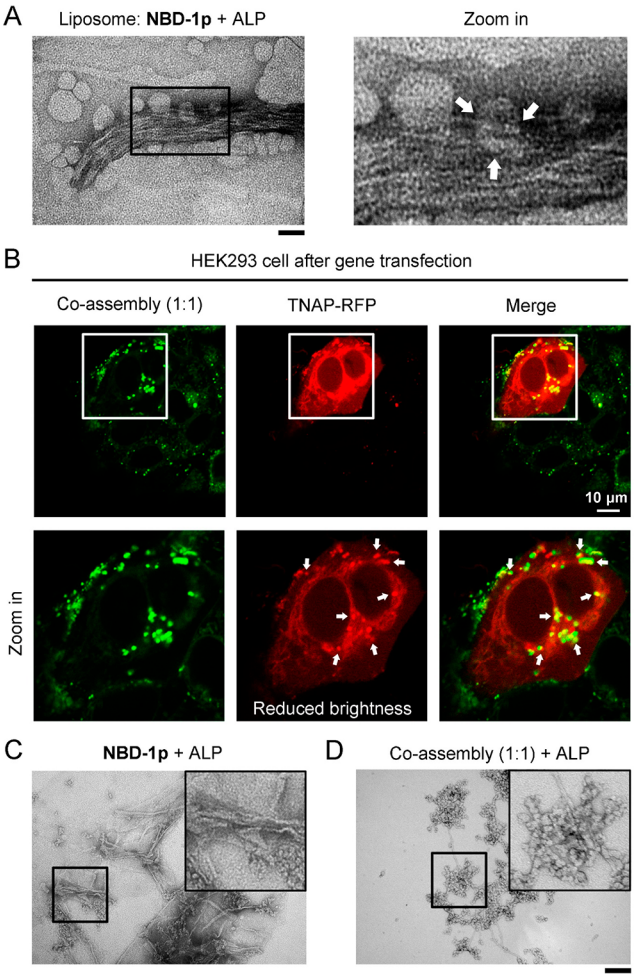

Figure 4. Coassembly of **NBD-1p** and **NBD-(D)Sp** shows less efficient endosomal escape. (A) TEM image of liposomes carrying **NBD-1p** and ALP (1 U/mL, 37 °C, 6 h). Broken liposomes are indicated by arrows. Scale bar = 100 nm. (B) Confocal fluorescence images of HEK293_TNAP-RFP cells incubated with the mixture of **NBD-1p** (100 μM) and **NBD-(D)Sp** (100 μM) for 12 h. The peptides trapped in endosome are indicated by arrows. (C) TEM images of **NBD-1p** (200 μM) and (D) the coassemblies of **NBD-1p** (100 μM) and **NBD-(D)Sp** (100 μM) after the addition of ALP (0.1 U/mL, 37 °C, 3 h) for partial dephosphorylation. ALP yields more nanofibers in panel C than in panel D. Scale bar = 100 nm.

nanofibers (**NBD-1**), which break the membrane of endocytic vesicles for escaping into cytosol. More TEM images reveal that the **NBD-1p** assemblies mixed with ALP initially remain as nanoparticles until a certain dephosphorylation ratio that triggers the particle-to-fiber phase transition (Figure S9 and Figure 3). This result implies that although dephosphorylation begins once TNAP binds to **NBD-1p** assemblies on the plasma membrane, the assemblies likely are maintained as nanoparticles (which consist of mainly **NBD-1p** and small amount **NBD-1**) during internalization until being further dephosphorylated in endosomal vesicles where nanofibers form for endosome rupturing. This observation also agrees with the reports that filamentous nanostructures have much reduced/limited cellular uptake ability relative to their spherical counterparts.[49,50]

https://doi.org/10.1021/acs.nanolett.1c01029
Nano Lett. 2021, 21, 4078−4085

To further prove the above assumption of endosomal escape, we incubate HEK293 cells, after TNAP-RFP gene transfection, with the mixture of **NBD-1p** and **NBD-(D)Sp** (total peptide concentration is 200 μM). The HEK293_TNAP-RFP cells incubated with the mixture of **NBD-1p** and **NBD-(D)Sp** at a 1:1 or 1:3 ratio mainly generate fluorescent puncta colocalizing with TNAP-RFP inside the cells (Figure 4B and Figure S10A), although the cells incubated with **NBD-1p** (100 or 50 μM) or **NBD-(D)Sp** (100 or 150 μM)), respectively, below CMC exhibit little fluorescence (Figure S11). This result indicates that **NBD-1p** and **NBD-(D)Sp** form coassemblies in solution, and the coassemblies of **NBD-1p** and **NBD-(D)Sp** (1:1 or 1:3) are primarily retained in the endocytic vesicles containing TNAP-RFP after the endocytosis. Our results also indicate that phosphopeptide assemblies exhibit emergent properties, which are absent in monomeric phosphopeptides. The nanoparticles formed by **NBD-1p** transform into nanofibers for endosomal rupturing after partial dephosphorylation by ALP (Figure 4C,D). Thus, the remaining phosphopeptides, after being released into cytosol, get further dephosphorylated by intracellular TNAP. This process produces networks of peptidic nanofibers that encapsulate intracellular TNAP (Figures 1D and 3A, TNAP colocalizes with NBD). However, the coassemblies of **NBD-1p** and **NBD-(D)Sp** (1:1 or 1:3) mixed with ALP mostly remain as nanoparticles (Figure 4D and Figure S10B) because **NBD-(D)Sp** is a poor substrate for ALP (Figure 3D). When the mixture has the ratio of **NBD-1p** and **NBD-(D)Sp** as 3:1, the coassemblies behave similarly to the assemblies of **NBD-1p** (Figure S10). Moreover, a phosphopeptide derivative (**NBD-3p**) carrying D-pTyr and pSer (Scheme S1) also ends up in the endosomal compartments of HEK293_TNAP-RFP cells after incubation (Figure S12). Like the coassemblies of **NBD-1p** and **NBD-(D)Sp** with a 1:1 or 1:3 ratio, **NBD-3P**, being treated by ALP, inefficiently undergoes the nanoparticle-to-nanofiber transition (Figure S13). This derivative also exhibits minimal cytotoxicity compared to other phosphopeptides (Figure S5). These results suggest that the particle-to-fiber transition of the phosphopeptide assemblies catalyzed by the ALP in the endosomes is critical for the endosomal escape of the peptide assemblies, likely via rupturing the endosome by the formation of nanofibers.

CONCLUSIONS

In conclusion, this work demonstrates that the continuous morphological transformation of peptide assemblies, catalyzed by ALP, is responsible for the endocytosis, mainly through the caveolae-mediated endocytic pathway, and endosomal escape of the peptide assemblies. Although other endocytosis pathways, such as macropinocytosis, may contribute to the cellular uptake of phosphopeptide assemblies, they are less likely to act as the main path for the phosphopeptide assemblies. Here, TNAP catalytically controls a dynamic morphological transition, thus enabling endocytosis and endosomal escape of peptide assemblies, in an analogy to the cell entry of the virus. Because **NBD-1p** mainly exists as nanoparticles at the concentration above the CMC, the effects of monomeric **NBD-1p** likely are insignificant. We suggest this type of cell uptake as "enzyme primed endocytosis (EPE)". While the contribution of VPP in the cell entry of the virus has been extensively studied, little research elucidates how EPE controls the cellular uptake of other molecular assemblies. In analogy to the ligand−receptor-mediated endocytosis that require tight binding, the clustering of enzymes in lipid rafts and the enzymatic reaction of supramolecular assemblies require rapid enzyme kinetics because **NBD-(D)Sp** hardly enters the cells. This study also provides a mechanistic understanding of the role of peptide assemblies for context-dependent signaling.[51,52] Although this work focuses on ALP and peptides, the mechanism revealed likely is applicable for the endocytosis of the substrates of esterase[53] or proteases,[54] including nonpeptide substrates of enzymes.

ASSOCIATED CONTENT

Supporting Information

The Supporting Information is available free of charge at https://pubs.acs.org/doi/10.1021/acs.nanolett.1c01029.

Experimental procedures, molecular structures, and additional results such as CMC values, viability assays, fluorescence imaging, LC−MS analysis, and TEM images (PDF)

Movie S1 showing the adherence of phosphopeptide assemblies on the plasma membrane of HEK293_TNAP-RFP cells, and the formation of more endocytic vesicles in HEK293_TNAP-RFP cells than in the nontransfected control (MP4)

Movie S2 showing intracellular fluorescence from NBD increasing significantly over time in the HEK293_TNAP-RFP cells, while remaining mostly unchanged in the nontransfected HEK293 cells (AVI)

Movie S3 showing that, below the CMC, the individual **NBD-1p** molecules do not aggregate on the plasma membrane of HEK293_TNAP-RFP cells (AVI)

AUTHOR INFORMATION

Corresponding Author

Bing Xu − *Department of Chemistry, Brandeis University, Waltham, Massachusetts 02453, United States;* orcid.org/0000-0002-4639-387X; Email: bxu@brandeis.edu

Authors

Hongjian He − *Department of Chemistry, Brandeis University, Waltham, Massachusetts 02453, United States*

Jiaqi Guo − *Department of Chemistry, Brandeis University, Waltham, Massachusetts 02453, United States*

Jiashu Xu − *Department of Chemistry, Brandeis University, Waltham, Massachusetts 02453, United States*

Jiaqing Wang − *Department of Chemistry, Brandeis University, Waltham, Massachusetts 02453, United States*

Shuang Liu − *Department of Chemistry, Brandeis University, Waltham, Massachusetts 02453, United States;* orcid.org/0000-0001-5548-8494

Complete contact information is available at: https://pubs.acs.org/10.1021/acs.nanolett.1c01029

Author Contributions

B.X. and H.H. designed the study. H.H. performed the experiment and generated the data. J.G. and J.X. assisted in the synthesis of peptides. J.W. and S.L. assisted in cell culture. B.X. and H.H. wrote the manuscript.

Notes

The authors declare no competing financial interest.

https://doi.org/10.1021/acs.nanolett.1c01029
Nano Lett. 2021, 21, 4078−4085

■ ACKNOWLEDGMENTS

The authors thank the NIH (R01CA142746) and NSF (DMR-2011846) for their support.

■ REFERENCES

(1) Overchuk, M.; Zheng, G. Overcoming obstacles in the tumor microenvironment: Recent advancements in nanoparticle delivery for cancer theranostics. *Biomaterials* **2018**, *156*, 217−237.
(2) Goswami, R.; Jeon, T.; Nagaraj, H.; Zhai, S.; Rotello, V. M. Accessing Intracellular Targets through Nanocarrier-Mediated Cytosolic Protein Delivery. *Trends Pharmacol. Sci.* **2020**, *41* (10), 743−754.
(3) Glass, Z.; Lee, M.; Li, Y.; Xu, Q. Engineering the Delivery System for CRISPR-Based Genome Editing. *Trends Biotechnol.* **2018**, *36* (2), 173−185.
(4) Futaki, S.; Suzuki, T.; Ohashi, W.; Yagami, T.; Tanaka, S.; Ueda, K.; Sugiura, Y. Arginine-rich peptides. An abundant source of membrane-permeable peptides having potential as carriers for intracellular protein delivery. *J. Biol. Chem.* **2001**, *276* (8), 5836−5840.
(5) MacEwan, S. R.; Chilkoti, A. Controlled apoptosis by a thermally toggled nanoscale amplifier of cellular uptake. *Nano Lett.* **2014**, *14* (4), 2058−2064.
(6) Lagerholm, B. C.; Wang, M.; Ernst, L. A.; Ly, D. H.; Liu, H.; Bruchez, M. P.; Waggoner, A. S. Multicolor coding of cells with cationic peptide coated quantum dots. *Nano Lett.* **2004**, *4* (10), 2019−2022.
(7) Tang, R.; Wang, M.; Ray, M.; Jiang, Y.; Jiang, Z.; Xu, Q.; Rotello, V. M. Active Targeting of the Nucleus Using Nonpeptidic Boronate Tags. *J. Am. Chem. Soc.* **2017**, *139* (25), 8547−8551.
(8) Wu, Y.; Zhang, L.; Cui, C.; Cansiz, S.; Liang, H.; Wu, C.; Teng, I. T.; Chen, W.; Liu, Y.; Hou, W.; Zhang, X.; Tan, W. Enhanced Targeted Gene Transduction: AAV2 Vectors Conjugated to Multiple Aptamers via Reducible Disulfide Linkages. *J. Am. Chem. Soc.* **2018**, *140* (1), 2−5.
(9) Zeng, H.; Little, H. C.; Tiambeng, T. N.; Williams, G. A.; Guan, Z. Multifunctional dendronized peptide polymer platform for safe and effective siRNA delivery. *J. Am. Chem. Soc.* **2013**, *135* (13), 4962−4965.
(10) Wang, Y.; Li, Z.; Shmidov, Y.; Carrazzone, R. J.; Bitton, R.; Matson, J. B. Crescent-Shaped Supramolecular Tetrapeptide Nanostructures. *J. Am. Chem. Soc.* **2020**, *142*, 20058−20065.
(11) Du, J. Z.; Du, X. J.; Mao, C. Q.; Wang, J. Tailor-Made dual pH-sensitive polymer-doxorubicin nanoparticles for efficient anticancer drug delivery. *J. Am. Chem. Soc.* **2011**, *133* (44), 17560−17563.
(12) June, R. K.; Gogoi, K.; Eguchi, A.; Cui, X. S.; Dowdy, S. F. Synthesis of a pH-sensitive nitrilotriacetic linker to peptide transduction domains to enable intracellular delivery of histidine imidazole ring-containing macromolecules. *J. Am. Chem. Soc.* **2010**, *132* (31), 10680−10682.
(13) Hu, Y.; Litwin, T.; Nagaraja, A. R.; Kwong, B.; Katz, J.; Watson, N.; Irvine, D. J. Cytosolic delivery of membrane-impermeable molecules in dendritic cells using pH-responsive core-shell nanoparticles. *Nano Lett.* **2007**, *7* (10), 3056−3064.
(14) He, H.; Liu, S.; Wu, D.; Xu, B. Enzymatically-Formed Peptide Assemblies Sequestrate Proteins and Relocate Inhibitors for Selectively Killing Cancer Cells. *Angew. Chem., Int. Ed.* **2020**, *59*, 16445−16450.
(15) Yan, R.; Hu, Y.; Liu, F.; Wei, S.; Fang, D.; Shuhendler, A. J.; Liu, H.; Chen, H. Y.; Ye, D. Activatable NIR Fluorescence/MRI Bimodal Probes for in Vivo Imaging by Enzyme-Mediated Fluorogenic Reaction and Self-Assembly. *J. Am. Chem. Soc.* **2019**, *141* (26), 10331−10341.
(16) He, H.; Tan, W.; Guo, J.; Yi, M.; Shy, A. N.; Xu, B. Enzymatic Noncovalent Synthesis. *Chem. Rev.* **2020**, *120* (18), 9994−10078.
(17) Feng, Z.; Wang, H.; Wang, F.; Oh, Y.; Berciu, C.; Cui, Q.; Egelman, E. H.; Xu, B. Artificial Intracellular Filaments. *Cell Rep. Phys. Sci.* **2020**, *1* (7), 100085.
(18) Zhan, J.; Cai, Y.; He, S.; Wang, L.; Yang, Z. Tandem Molecular Self-Assembly in Liver Cancer Cells. *Angew. Chem., Int. Ed.* **2018**, *57* (7), 1813−1816.
(19) Chang, J.; Cai, W.; Liang, C.; Tang, Q.; Chen, X.; Jiang, Y.; Mao, L.; Wang, M. Enzyme-Instructed Activation of Pro-protein Therapeutics in Vivo. *J. Am. Chem. Soc.* **2019**, *141* (45), 18136−18141.
(20) Yuan, Y.; Wang, L.; Du, W.; Ding, Z.; Zhang, J.; Han, T.; An, L.; Zhang, H.; Liang, G. Intracellular self-assembly of Taxol nanoparticles for overcoming multidrug resistance. *Angew. Chem., Int. Ed.* **2015**, *54* (33), 9700−9704.
(21) Wu, C.; Zhang, R.; Du, W.; Cheng, L.; Liang, G. Alkaline phosphatase-triggered self-assembly of near-infrared nanoparticles for the enhanced photoacoustic imaging of tumors. *Nano Lett.* **2018**, *18* (12), 7749−7754.
(22) Hai, Z.; Ni, Y.; Saimi, D.; Yang, H.; Tong, H.; Zhong, K.; Liang, G. γ-glutamyltranspeptidase-triggered intracellular gadolinium nanoparticle formation enhances the T2-weighted MR contrast of tumor. *Nano Lett.* **2019**, *19* (4), 2428−2433.
(23) Li, G.; Hu, X.; Nie, P.; Mang, D.; Jiao, S.; Zhang, S.; Roy, S. R.; Yukawa, S.; Asahina, S.; Sugasawa, H.; Cortes, W.; Zhou, Z.; Zhang, Y. Lipid-Raft-Targeted Molecular Self-Assembly Inactivates YAP to Treat Ovarian Cancer. *Nano Lett.* **2021**, *21*, 747−755.
(24) Tan, X.; Li, B. B.; Lu, X.; Jia, F.; Santori, C.; Menon, P.; Li, H.; Zhang, B.; Zhao, J. J.; Zhang, K. Light-triggered, self-immolative nucleic acid-drug nanostructures. *J. Am. Chem. Soc.* **2015**, *137* (19), 6112−6115.
(25) Wei, T.; Lu, S.; Sun, J.; Xu, Z.; Yang, X.; Wang, F.; Ma, Y.; Shi, Y. S.; Chen, X. Sanger's Reagent Sensitized Photocleavage of Amide Bond for Constructing Photocages and Regulation of Biological Functions. *J. Am. Chem. Soc.* **2020**, *142* (8), 3806−3813.
(26) Feng, Z.; Han, X.; Wang, H.; Tang, T.; Xu, B. Enzyme-instructed peptide assemblies selectively inhibit bone tumors. *Chem.* **2019**, *5* (9), 2442−2449.
(27) Zhou, J.; Du, X.; Chen, X.; Wang, J.; Zhou, N.; Wu, D.; Xu, B. Enzymatic self-assembly confers exceptionally strong synergism with NF-κB targeting for selective necroptosis of cancer cells. *J. Am. Chem. Soc.* **2018**, *140* (6), 2301−2308.
(28) Zhan, J.; Cai, Y.; He, S.; Wang, L.; Yang, Z. Tandem molecular self-assembly in liver cancer cells. *Angew. Chem.* **2018**, *130* (7), 1831−1834.
(29) Ou, X.; Liu, Y.; Lei, X.; Li, P.; Mi, D.; Ren, L.; Guo, L.; Guo, R.; Chen, T.; Hu, J.; et al. Characterization of spike glycoprotein of SARS-CoV-2 on virus entry and its immune cross-reactivity with SARS-CoV. *Nat. Commun.* **2020**, *11* (1), 1620−12.
(30) Parton, R. G.; Joggerst, B.; Simons, K. Regulated internalization of caveolae. *J. Cell Biol.* **1994**, *127* (5), 1199−1215.
(31) Dube, D.; Brecher, M. B.; Delos, S. E.; Rose, S. C.; Park, E. W.; Schornberg, K. L.; Kuhn, J. H.; White, J. M. The primed ebolavirus glycoprotein (19-Kilodalton GP 1,2): Sequence and residues critical for host cell binding. *J. Virol.* **2009**, *83* (7), 2883−2891.
(32) Hoffmann, M.; Kleine-Weber, H.; Schroeder, S.; Kruger, N.; Herrler, T.; Erichsen, S.; Schiergens, T. S.; Herrler, G.; Wu, N. H.; Nitsche, A.; Muller, M. A.; Drosten, C.; Pohlmann, S. SARS-CoV-2 Cell Entry Depends on ACE2 and TMPRSS2 and Is Blocked by a Clinically Proven Protease Inhibitor. *Cell* **2020**, *181* (2), 271−280.
(33) Wu, H.; Fuxreiter, M. The structure and dynamics of higher-order assemblies: amyloids, signalosomes, and granules. *Cell* **2016**, *165* (5), 1055−1066.
(34) Wang, Q.; Jiang, N.; Fu, B.; Huang, F.; Liu, J. Self-assembling peptide-based nanodrug delivery systems. *Biomater. Sci.* **2019**, *7* (12), 4888−4911.
(35) Li, J.; Kuang, Y.; Shi, J.; Zhou, J.; Medina, J. E.; Zhou, R.; Yuan, D.; Yang, C.; Wang, H.; Yang, Z.; et al. Enzyme-instructed intracellular molecular self-assembly to boost activity of cisplatin against drug-resistant ovarian cancer cells. *Angew. Chem., Int. Ed.* **2015**, *54* (45), 13307−13311.

https://doi.org/10.1021/acs.nanolett.1c01029
Nano Lett. 2021, 21, 4078−4085

(36) Thomas, P.; Smart, T. G. HEK293 cell line: a vehicle for the expression of recombinant proteins. *J. Pharmacol. Toxicol. Methods* **2005**, *51* (3), 187−200.
(37) Longo, P. A.; Kavran, J. M.; Kim, M.-S.; Leahy, D. J. Transient mammalian cell transfection with polyethylenimine (PEI). In *Methods in Enzymology*; Elsevier, 2013; Vol. *529*, pp 227−240.
(38) Lin, C.; Sasaki, M.; Orcutt, M.; Miyayama, H.; Singer, R. Plasma membrane localization of alkaline phosphatase in HeLa cells. *J. Histochem. Cytochem.* **1976**, *24* (5), 659−667.
(39) De Broe, M. E.; Roels, F.; Nouwen, E. J.; Claeys, L.; Wieme, R. J. Liver plasma membrane: the source of high molecular weight alkaline phosphatase in human serum. *Hepatology* **1985**, *5* (1), 118−128.
(40) Le, P. U.; Guay, G.; Altschuler, Y.; Nabi, I. R. Caveolin-1 is a negative regulator of caveolae-mediated endocytosis to the endoplasmic reticulum. *J. Biol. Chem.* **2002**, *277* (5), 3371−3379.
(41) Mahammad, S.; Parmryd, I., Cholesterol depletion using methyl-β-cyclodextrin. In *Methods in Membrane Lipids*; Springer, 2015; pp 91−102.
(42) Milhiet, P. E.; Giocondi, M. C.; Baghdadi, O.; Ronzon, F.; Roux, B.; Le Grimellec, C. Spontaneous insertion and partitioning of alkaline phosphatase into model lipid rafts. *EMBO Rep.* **2002**, *3* (5), 485−490.
(43) Dahl, R.; Sergienko, E. A.; Su, Y.; Mostofi, Y. S.; Yang, L.; Simao, A. M.; Narisawa, S.; Brown, B.; Mangravita-Novo, A.; Vicchiarelli, M.; et al. Discovery and validation of a series of aryl sulfonamides as selective inhibitors of tissue-nonspecific alkaline phosphatase (TNAP). *J. Med. Chem.* **2009**, *52* (21), 6919−6925.
(44) Müller, A.; Klöppel, C.; Smith-Valentine, M.; Van Houten, J.; Simon, M. Selective and programmed cleavage of GPI-anchored proteins from the surface membrane by phospholipase C. *Biochim. Biophys. Acta, Biomembr.* **2012**, *1818* (1), 117−124.
(45) Vasile, E.; Simionescu, M.; Simionescu, N. Visualization of the binding, endocytosis, and transcytosis of low-density lipoprotein in the arterial endothelium in situ. *J. Cell Biol.* **1983**, *96* (6), 1677−1689.
(46) Goldstein, J. L.; Anderson, R.; Brown, M. S. In *Receptor-mediated endocytosis and the cellular uptake of low density lipoprotein. Ciba Foundation symposium* **2008**, 77−95.
(47) Goldstein, J. L.; Brown, M. S.; Anderson, R. G.; Russell, D. W.; Schneider, W. J. Receptor-mediated endocytosis: concepts emerging from the LDL receptor system. *Annu. Rev. Cell Biol.* **1985**, *1* (1), 1−39.
(48) V'kovski, P.; Kratzel, A.; Steiner, S.; Stalder, H.; Thiel, V. Coronavirus biology and replication: implications for SARS-CoV-2. *Nat. Rev. Microbiol.* **2021**, *19*, 155−170.
(49) Lock, L. L.; Reyes, C. D.; Zhang, P.; Cui, H. Tuning cellular uptake of molecular probes by rational design of their assembly into supramolecular nanoprobes. *J. Am. Chem. Soc.* **2016**, *138* (10), 3533−3540.
(50) Nishiyama, N. Nanocarriers shape up for long life. *Nat. Nanotechnol.* **2007**, *2* (4), 203−204.
(51) Wang, H.; Feng, Z.; Xu, B. Instructed Assembly as Context-Dependent Signaling for the Death and Morphogenesis of Cells. *Angew. Chem., Int. Ed.* **2019**, *58* (17), 5567−5571.
(52) Shang, Y.; Zhi, D.; Feng, G.; Wang, Z.; Mao, D.; Guo, S.; Liu, R.; Liu, L.; Zhang, S.; Sun, S.; et al. Supramolecular nanofibers with superior bioactivity to insulin-like growth factor-I. *Nano Lett.* **2019**, *19* (3), 1560−1569.
(53) Mix, K. A.; Lomax, J. E.; Raines, R. T. Cytosolic delivery of proteins by bioreversible esterification. *J. Am. Chem. Soc.* **2017**, *139* (41), 14396−14398.
(54) Tanaka, A.; Fukuoka, Y.; Morimoto, Y.; Honjo, T.; Koda, D.; Goto, M.; Maruyama, T. Cancer cell death induced by the intracellular self-assembly of an enzyme-responsive supramolecular gelator. *J. Am. Chem. Soc.* **2015**, *137* (2), 770−775.

https://doi.org/10.1021/acs.nanolett.1c01029
Nano Lett. 2021, 21, 4078−4085